

# Facial Age Simulation using Age-specific 3D Models and Recursive PCA

Anastasios Maronidis and Andreas Lanitis

*Department of Multimedia and Graphic Arts, Cyprus University of Technology, P.O. Box 50329, 3036 Lemessos, Cyprus*

**Keywords:** Age Simulation, Age Specific Statistical Models, Recursive PCA, Anthropometric Measurements.

**Abstract:** Facial age simulation is a topic that has been gaining increasing interest in computer vision. In this paper, a novel age simulation method that utilizes age-specific shape and texture models is proposed. During the process of generating age-specific shape models, 3D face measurements acquired from real human faces are used in order to tune a generic 3D face shape model to represent face shapes belonging to certain age groups. A number of diagnostic studies have been conducted in order to validate the compatibility of the tuned shape models with the corresponding age groups. The shape age-simulation process utilizes age-specific shape models that incorporate age-related constraints during a 3D shape reconstruction phase. Age simulation is completed by predicting the texture at the target age based on a recursive PCA method that aims to superimpose age-related texture modifications in a way that preserves identity-related characteristics of the subject in the source image. Preliminary results indicate the potential of the proposed method.

## 1 INTRODUCTION

Age simulation can prove an important task in a broad range of applications such as the prediction of facial appearance of missing persons, automated update of records, face recognition robust to aging variation, entertainment applications and cosmetology. Simulating facial aging is a tough problem due to the diversity of aging variation for different subjects and the dependence of the aging process on external factors related to a person's lifestyle.

Many studies related to face age progression have shown that different mechanisms are responsible for the aging of shape and texture. Particularly, in formative years a face is predominantly subjected to shape transformations, while in adulthood the main changes are expressed as texture transformations (Fu et al., 2010).

The contribution of this work is an integrated system, which given a person's face that belongs to a certain age group, it predicts its shape and texture in a target age group. Despite the fact that in the past age progression techniques that combine shape and texture manipulations were reported (Du et al., 2012), (Lanitis et al., 2002), (Park et al., 2008) in our method, shape and texture information is treated separately through the use of age specific 3D shape

and texture models. Using 3D instead of 2D models enables the application of the proposed method on faces with different orientations.

During the training phase a set of anthropometric face measurements (Farkas, 1994) in conjunction with a generic 3D face Point Distribution Model (PDM) (Cootes et al., 1995) are used in order to generate 3D PDM's specific for each age group. The method for generating age-specific shape models is based on our previous work (Lanitis et al., 2012) where a set of stylistic rules are used for tuning a generic 3D shape model to a certain design style. In the case of texture, age-specific models are trained using texture samples extracted from faces belonging to different age groups.

During the age simulation phase the age-transformed shape of the target face is obtained by 3D reconstructing the raw face using a 3D shape model specific to the target age group. The use of an age-group specific PDM ensures that during the 3D reconstruction phase age-specific constraints are enforced so that the resulting shape possesses characteristics compatible with the target age group. The texture of the resulting 3D face is segmented into two equal parts with respect to the vertical axis of face symmetry. Keeping the one out of the two halves intact and considering the second half occluded, the 3D target face is predicted by utilizing



vector, where each element contains the mean value of the corresponding measurement among the overall population of that age group. Given an arbitrary synthetic 3D face shape instance it is possible to use the vertex coordinates for measuring the values of the six measurements in question and subsequently estimate the distance of the face instance from each of the seven age groups.



Figure 2: The 6 anthropometric head measurements. From left to right: Bigonial Width, Bizygomatic Breadth, Head Breadth, Menton-Sellion, Minimum Frontal and Nose Width.

With the help of a generic 3D PDM trained with laser scanned 3D faces (Blanz et al., 1999), using an exhaustive grid search over the PDM parameters, we generate synthetic face instances. For each of these instances, we estimate the values of the six anthropometric measurements so that a 6-dimensional feature vector representing the face instance is created. The Euclidean distance of this feature vector from each one of the seven age group mean vectors is then calculated and used as the discrepancy measure. The face instance is finally assigned to the nearest age group since it mostly complies with this group.

Having obtained a set of 60 compliant samples for each age group, we train a corresponding 3D PDM. These PDM's convey statistical information relevant to the faces of that age, with respect to their shape. Therefore, reconstructing a 2D face using an age specific PDM has the advantage that the resulting face should contain shape information of both the id and the age group.

### 3.2 Diagnostic Tests

A series of diagnostic tests has been conducted in order to verify the compatibility of the generated 3D PDM's to the corresponding age groups. Tests have been carried out using synthetic and real samples.

#### 3.2.1 Age Group Discrepancies

**Experiments using Synthetic Faces:** Using the 3D PDM that corresponds to the 2-6 yrs age group trained above, we generate 1000 random 3D face shape instances. For each synthetic face instance we estimate the values of the six face measurements (see Fig. 2) and calculate the discrepancy of the

synthetic sample from each age group. As stated in section 3.1 the discrepancy is defined as the Euclidean distance of the six measurements and the mean values for each age group. The distributions of the discrepancies of instances generated using the 3D PDM that corresponds to the 2-6 yrs age group from each of the seven age groups are plotted in Fig. 3. Discrepancy is depicted in the x-axis. It is clear that face instances that have been generated by the 2-6 yrs PDM have the lowest discrepancy from the 2-6 yrs age group.

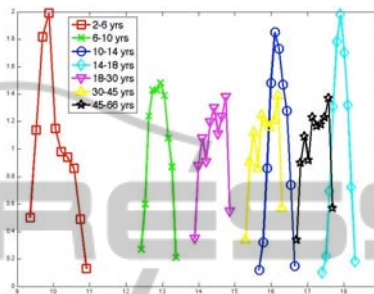


Figure 3: Distribution of discrepancies of instances generated by 2-6 yrs 3D PDM from the seven age groups (seven curves).

Similar but less pronounced results were obtained when the same test was repeated using the 3D PDM's for different age groups. This finding corroborates the claim that shape changes in human face mainly take place during formative years. The overall results show in a clear way that instances generated by an age specific PDM mostly comply with the corresponding age group.

**Experiments using Real Faces:** Using the FG-NET (<http://fgnet.rsunit.com>) aging database, the faces of a certain age group are 3D reconstructed by using each of the seven age group specific 3D PDM's. Thus, seven types of 3D reconstruction of the faces from the age group in question are obtained. 3D reconstruction has been accomplished by utilizing a method similar to the one proposed in (Blanz et al., 2004). For each reconstruction type, the mean discrepancy of the corresponding 3D reconstructed faces from the age group in question has been calculated. This process has been applied to all age groups. The results for the age groups 2-6, 6-10, 10-14 and 14-18 yrs old are illustrated in Fig. 4. The corresponding bar diagrams for the remaining age groups have been omitted because they are almost identical to that of 14-18.

In almost all the cases, samples that belong to the same age group as the age group specific PDM return the lowest total discrepancy. This is another

way to ensure that the PDM's that correspond to an age group are indeed compatible with that age group. The difference of the mean discrepancy between the age group in question and the remaining age groups is clearly more pronounced in the first two diagrams. As the age progresses, the mean discrepancies become more uniformly distributed. This result emphasizes the increased intensity of shape changes during the formative years.

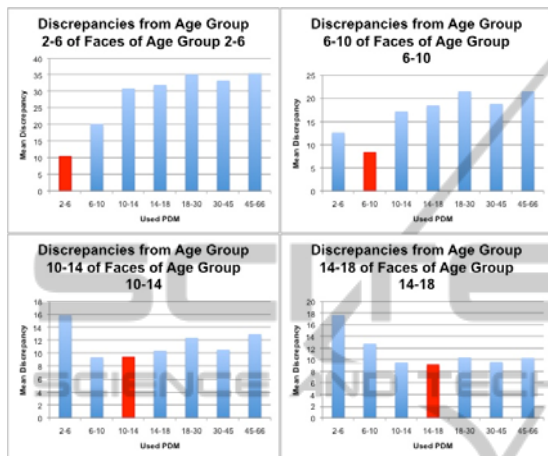


Figure 4: Bar diagrams of mean discrepancies from the age groups 2-6, 6-10, 10-14 and 14-18 of faces belonging to these age groups reconstructed using different 3D PDM's. The 3D PDM that corresponds to the age group in question is depicted with red.

### 3.2.2 Age Classification

**Experiments using Synthetic Faces:** Using the 6-measurement representation of 100 random instances generated by each of the seven age-group specific PDM's, we have conducted an age classification experiment using five-fold cross validation (CV). For classifying the samples, a minimum Mahalanobis distance classifier has been used. The average correct classification train and test rates through the 5 CV steps are depicted in the first row of Table 1. The 100% classification rates obtained indicate that the six measurements offer a reasonable representation for discriminating face instances produced by different age-group specific shape models.

**Experiments using Real Samples:** We have 3D reconstructed the faces depicted in FG-NET dataset employing a method similar to the one proposed in (Blanz et al., 2004). For this purpose, we have used both a generic 3D PDM and each of the age group specific 3D PDM's. Using again the six measurements as feature representation we have performed classification with respect to age. The

classification settings are the same as in the experiment using synthetic faces. The results using the generic and the Age Group Specific (AGS) PDM's are shown in the second and third rows of Table 1, respectively.

Table 1: Results of age classification experiments.

	Train Rate (%)	Test Rate (%)
Synthetic faces	100.0	100.0
FGNET using generic PDM	69.2	52.7
FGNET using AGS PDM	100.0	99.7

Comparing these two rows it can be easily observed that using age specific PDM's returns approximately double accuracy rate than using generic PDM implying that unlike the generic 3D PDM, age specific 3D PDM's retain age-related information during the 3D reconstruction process. Despite the quite high accuracy rate obtained by using age specific PDM's, it must be stated that this is just a diagnostic test assessing the specificity of the generated models to each age group. The aforementioned techniques cannot be treated as age estimation results, since during the 3D reconstruction process of FG-NET images we use the a priori information in selecting the appropriate age group specific 3D PDM for each face instance. Nevertheless, this test accentuates the significance of age group specific 3D PDM's in representing real faces of different ages.

## 4 AGE SIMULATION

Given a face image that shows a subject at a certain age, we attempt to predict the appearance of the same person in a target age. Using the Target Age Group Specific (TAGS) 3D PDM trained in the way described in the previous section, we estimate firstly the shape of the target face. We also train a TAGS texture PCA model using samples belonging to the target age group—from the FG-NET aging database. Using this model, we estimate the texture of the target face using the method described in 4.2.

### 4.1 Shape

Given a raw face, we locate 68 landmarks, which correspond to some predefined salient facial features, (Lanitis et al., 2002). Using these landmarks along with the trained TAGS 3D shape model, we reconstruct the 3D version of the initial 2D face image. The resulted 3D face shape approximates the corresponding face shape of the

given subject at the target age group, because the age specific shape model contain statistical information from that age group. This claim is substantiated by the experimental results reported in section 3.2.

## 4.2 Texture

For predicting the texture of a raw face at the target age, we use a modified version of the recursive PCA method (Park et al., 2003), (Wang et al., 2007). Recursive PCA is a technique used extensively for restoring partially damaged or occluded face images. During the training phase, each sample from the FG-NET aging database is 3D reconstructed using the 3D PDM that corresponds to the age group in which the sample belongs to. Using the 3D reconstructed samples, a Principal Component Analysis (PCA) texture model for each age group is trained.

During age simulation, a raw face is 3D reconstructed and divided into two equal segments with respect to the vertical axis of face symmetry. The one out of the two halves is used as the reference part of the face, while the second half is used as the control part. At each iteration, the whole face is coded into TAGS texture model parameters and back reconstructed in the face space. This code-reconstruction scheme produces a new face. The distance between the two faces is defined as the summation of the absolute differences of the intensities of the vertices that belong to the control part of the two faces. If this value is minimized, the process is completed and the simulated face is the reconstructed one. Otherwise, the reference part of the reconstructed face is replaced by the corresponding part of the initial raw face and the process is repeated.

The rationale behind this approach is to exploit the statistical texture information about the target age group contained in the texture model, as well as to maintain information about the id through the use of the original half. Therefore, it is expected that the resulting face comprises a prediction of the actual appearance of the id at the target age.

Indicative examples of both forward and reverse age texture simulation are provided in Fig. 5. In Fig. 5 the leftmost picture is the raw face, the middle picture comprises a mixture of the raw and the age-transformed face and the rightmost picture consists of the whole predicted face texture in the target age group. In Fig. 5, by comparing the initial with the reconstructed part it can be stated that the identity is maintained in a high degree. Moreover, texture characteristics pertaining to the target age group are

also embedded in the reconstructed part. Examples of the application of the combined shape and texture age simulation methodology in forward and reverse age progression are provided in Fig. 6.



Figure 5: Facial texture simulation 5 to 45-66 yrs old (top) and 50 to 2-6 yrs old (bottom).

## 5 CONCLUSIONS

In this work, an integrated technique for simulating facial age progression has been proposed. The major contribution of the proposed method is the separate use of both shape and texture age specific statistical models. The problem of incomplete existing datasets inhibits the training of statistical shape models that represent the several age groups. For this purpose, anthropometric measurements have been utilized for tuning a generic statistical shape model into several age-specific ones. A comprehensive diagnostic study of the proposed technique has also been performed giving promising results. Preliminary visual results obtained by using the proposed method have been provided for visual inspection in order to extract some intuitive findings.

The work is still in process. As part of our plans for future work we plan to conduct further diagnostic studies with respect to the use of the recursive PCA method for age simulation. We also plan to stage systematic performance evaluation experiments for assessing the age progression results using dedicated performance evaluation methods (Lanitis, 2008). In addition an extended aging dataset (Ricanek et al., 2006) will be employed so that more representative age specific texture models are utilized during the texture age simulation process.

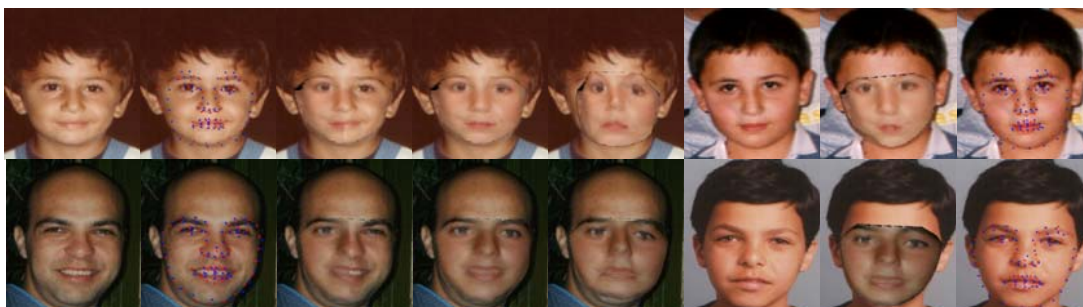


Figure 6: Forward age progression from 3 to 10 yrs old (top row) and reverse age progression from 12 to 4 yrs old (bottom row). From left to right the raw image, initial (red) and reconstructed (blue) landmarks overlaid on raw image, half predicted image warped on raw image, total predicted image warped on raw image, total predicted image overlaid on raw image (no warping), real face image at the target age, predicted image warped on target image, initial (red) and reconstructed (blue) target image landmarks overlaid on target image are shown.

## ACKNOWLEDGEMENTS

Part of the work presented was supported by the Cyprus Research Promotion Foundation and the European Union Structural Funds (project T1IE/Π1AHPO/0609(BIE)/05)

## REFERENCES

- Blanz, V., Vetter, T., A Morphable Model for the Synthesis of 3D Faces, In *Computer Graphics, Annual Conference Series (SIGGRAPH)*, pp. 187-194, 1999.
- Blanz, V., Mehler, A., Vetter T. and Seidel H., A Statistical Method for Robust 3d Surface Reconstruction From Sparse Data, In *Proc. Intl. Symposium on 3D Data Processing, Visualization and Transmission*, 2004.
- Cootes, T. F., Taylor, C. J., Cooper, D. H., Graham, J., Active Shape Models - Their Training and Application, *Computer Vision and Image Understanding*, Vol. 61, No. 1, pp. 38-59, Jan. 1995.
- Du, J.-X., Zhai, C.-M., Ye, Y.-Q., Face aging simulation based on NMF algorithm with sparseness constraints, *Proc. of the 7th Intl. Conf. on Advanced Intelligent Computing Theories and Applications: with aspects of artificial intelligence*, Springer Berlin / Heidelberg, vol. 6839, pp. 516-522, 2012.
- Farkas, L. G., *Anthropometry of the Head and Face*, Raven Press, New York, 1994.
- Fu, Y., Guo, G., Huang, T.S., Age Synthesis and Estimation via Faces: A Survey, *IEEE Trans. Pattern Anal. Mach. Intell.*, vol. 32, no. 11, pp. 1955-1976, Nov. 2010.
- Goldstein, M. S., Changes in dimensions and form of the face and head with age, *Am J Phys Anthropol*, 22:37-89, 1936.
- Lanitis, A., Taylor, C. J. and Cootes, T. F., Toward Automatic Simulation Of Aging Effects on Face Images. *IEEE Trans. of Pattern Analysis and Machine Intelligence*, Vol 24, no 4, pp 442-455, 2002.
- Lanitis, A., Evaluating the Performance of Face-Aging Algorithms. *Procs. of the IEEE Intl. Conf. on Face and Gesture Recognition*, 2008.
- Lanitis, A., Stylianou, G., Voutounos C., Virtual Restoration of Faces Appearing In Byzantine Icons, *International Journal of Cultural Heritage*, Elsevier, (doi:10.1016/j.culher.2012.01.001), 2012.
- Park, J.-S., Oh, Y.-H., Ahn, S.-C., Lee, S.-W., Glasses Removal from Facial Image Using Recursive PCA Reconstruction, *Intl Conf. Audio and Video-based Biometric Person Authentication*, pp. 369-376, 2003.
- Park, U., Tong, Y., Jain, A. K., Face recognition with temporal invariance: A 3d aging model, *IEEE Intl. Conf. on Face and Gesture Recognition*, 2008.
- Ramanathan, N., Chellappa, R., Biswas, S., Computational Methods for Modeling Facial Aging: A Survey, *J. Visual Languages and Computing*, vol. 20, no. 3, pp. 131-144, 2009.
- Ramanathan, N., Chellappa, R., Modeling Age Progression in Young Faces, *Proc. IEEE Conf. Computer Vision and Pattern Recognition*, pp. 387-394, 2006.
- Ricanek, K., Tesafaye, T., MORPH A Longitudinal Image Database of Normal Adult Age-Progression. *Procs. of the 7th IEEE Intl. Conf. on Face and Gesture Recognition*, pp. 341-345, 2006.
- Wang, Z. M., Tao, J.H., Reconstruction of Partially Occluded Face by Fast Recursive PCA, *Int. Conf. on Computational Intelligence and Security Workshops*, Harbin, December 15-19, 2007.
- Zhuang, Z., Bradtmiller, B., Head and face anthropometric survey of U.S. respirator users, *J. Occup. Environ. Hyg.*, 2, 567-576, 2005.